IOP Conf. Series: Materials Science and Engineering **655** (2019) 012001 doi:10.1088/1757-899X/655/1/012001

The effect of cast structures on texture and mechanical properties of AISI 433 ferritic stainless steel

[1, 2] M Maumela, [1]W E Stumpf, [1] C W Siyasiya

[1] The University of Pretoria, Department of Material Science & Metallurgical Engineering, Private Bag X20, Hatfield Campus, Pretoria 0028, South Africa, Tel. +2712 420 3182

[2] Mintek, Advanced Materials Division, Private Bag X3015, Randburg, 2125, South Africa, Tel. +2711 709 4462

E-mail address: mbavhalelom@mintek.co.za

Abstract: The influence of the individual equiaxed and columnar cast structure on the evolution of texture during thermo-mechanical processes (TMP) was investigated using the electron backscatter diffraction (EBSD) technique. The recrystallization texture after cold working and annealing was then related to mechanical properties of the initial cast structures. It was found that the initial equiaxed cast structure exhibited a homogenous $\gamma-$fiber texture while the columnar developed an inhomogeneous texture with the predominance of both the Goss and $\alpha-$fiber textures. While texture has a significant influence on surface smoothness of the drawn product, it was found that it did not significantly affect the yield strength and ultimate tensile strength (UTS), but marginally affected the elongation i.e. it was found to be slighted higher for the equiaxed than the columnar cast structure measured parallel to the rolling direction (RD).

1. Introduction

The ferritic stainless steel (FSS) AISI 433 is a newly developed grade from a parent grade AISI 430 through micro-alloying with Al. Its demand has increased for replacing expensive austenitic stainless in some engineering applications where corrosion resistance is a primary requirement. However, it is highly prone to surface ridging defects under tensile forming operations. It also has limited drawability compared to austenitic grades.

The ridging phenomenon is associated with grain colonies or clusters which exhibit heterogeneous crystallographic texture distribution in finished rolled sheet products and is only manifested when the product is subjected to a tensile strain during forming operation [1]. When the sheet is subjected to at least 10% tensile elongation, the surface displays narrow corrugated ridges, with an average of 50 μm height peaks on one side of the sheet surface coinciding with troughs on the opposite side, aligned parallel to the RD (rolling direction) [2, 3]. This behaviour is undesirable in the use of aesthetic design where surface quality is highly considered.

It has been reported that surface ridging resistance and formability are improved through recrystallized homogeneous $\gamma-$fiber texture components on the final sheet product and this is contrary to the heterogeneous distribution of texture, which degrade these properties [3]. The heterogeneous texture distribution is developed from the initial as-cast columnar structures (ICCS) texture, $\{100\}//ND$ (normal direction), during the TMP i.e. it develops into the $\alpha-$fiber, $\gamma-$fibre and, Goss texture components. However, the initial as-cast equiaxed structures (IECS) exhibits random texture which leads to the homogeneous $\gamma-$fiber texture after TMP [4]. The random texture of equiaxed solidification structures and elongated columnar structure with $\{100\}//ND$ were confirmed by Sudipta et al. [2]. Kim et al. [5] applied electromagnetic stirring (EMS) in continuous casting to suppress the

Content from this work may be used under the terms of the Creative Commons Attribution 3.0 licence. Any further distribution of this work must maintain attribution to the author(s) and the title of the work, journal citation and DOI.
Published under licence by IOP Publishing Ltd

columnar grains with $< 001 >$//ND orientations and instead promote the grain refinement and the equiaxed grains with random texture in order to improve ridging resistance of FSS sheet.

In this study, the effect of the individual IECS versus ICCS on texture evolution during rolling and annealing process was investigated. The observed recrystallized textures were then related to the mechanical properties, by plotting stress-strain curves.

2. Experimental procedure

Industrially produced as cast steel slab sample, 200 mm thickness and of the chemical composition in Table 1, was supplied by Columbus Stainless (SA). The slab sample was ground using 2400 grit on both opposite cross-sectioned surfaces and micro-etched with aqua regia solution to reveal solidification structures. Zones containing equiaxed and columnar solidification structures were mechanically separated into equal size blocks with a thickness of 25.5 mm.

Table 1. Chemical composition of the steel slab of AISI 433

Element	**C**	N	**Cr**	**Ni**	Mn	Si	Cu	V	**Al**	Nb	Fe
Mass %	**0.048 max**	0.037	**16.40**	**0.160**	0.510	0.290	0.090	0.120	**0.261**	0.002	Bal.

The industrial hot rolling process was simulated as shown in figure.1 overleaf. Thereafter, both the ICCS and IECS strips were cold rolled 62 % to 1.5 mm final thickness and annealed at 900 ℃ for 3 minutes then water quenched. Samples for metallurgical analysis were obtained after each rolling stage.

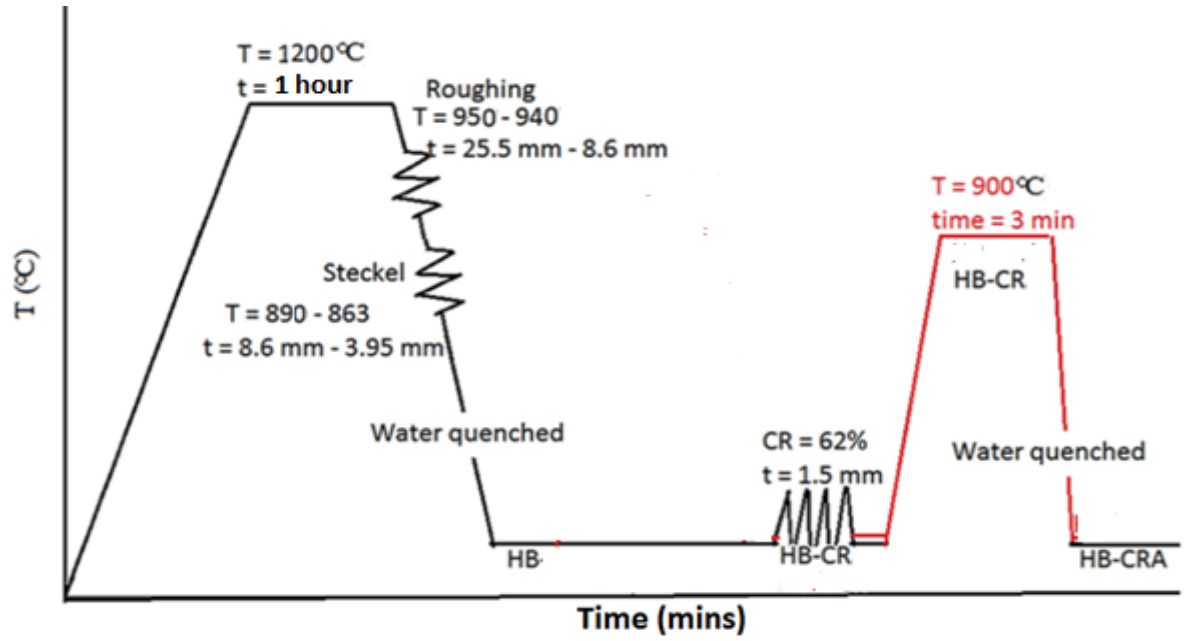

Figure 1. Thermo-mechanical schedule applied to the sample

The texture analysis was performed on the rolling plane (RD-TD) and was measured by the SEM-EBSD technique. The results were presented in Orientation Distribution Function (ODF) at section $\varphi_2 = 45°$, Bunge notation, see figure 2. Tensile testing was performed after cold working and annealing (HB-CRA) according to ASTM E 8 sub-standard (gauge length of 50 mm, thickness of 1.5 mm and width of 20 mm). Three tensile specimen were pulled in the RD per sample at a cross head speed of 2 mm/minute in an Instron Model 1175 machine. The strain was measured by using strain gauge device, attached on specimen gauge length. The specimens were pulled until fracture.

The section ($\varphi_2 = 45°$) was selected because it defines almost all bcc steel fiber texture components, that form during processing of steel, i.e. casting, rolling and annealing processing stages. The fiber texture components were mainly α −fiber, γ −fiber, Goss, Cube texture, rotated Cube texture and other texture components as are shown in figure 2.

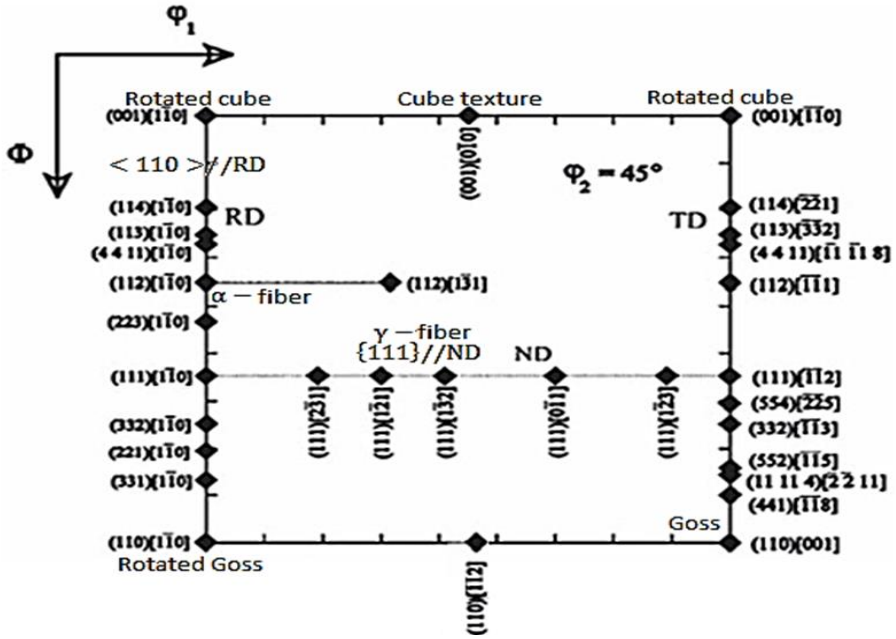

Figure 2. Ideal texture components located at ODF $\varphi_2 = 45°$ section of bcc steels

3. Results and Discussion

3.1. Cold rolling (HB-CR) texture

Figure 3 shows the ODFs for the IECS and ICCS after cold rolling (HB-CR). As may be seen, the IECS exhibited a strong γ −fibre texture components and a weak Cube texture. On the contrary, the ICCS attained two main texture components with the exception of the desired γ −fibre texture components, i.e. rotated Cube texture components with 3.574/4.011 intensity and followed by $(112)[1\bar{3}1]$ with 2.770/4.011 intensity, figure.3 (b). In other words, unlike the IECS, the ICCS promoted heterogeneous texture distribution. The IECS strongly oriented (111)-grains, which could be attributed to the pre-existing hot band (111)-grain orientations as a result of a random as-cast texture in equiaxed as-cast structures [1]. The (111)-orientation is known to store a larger amount of deformation energy than any other orientation and, therefore influences the neighbouring grains to rotate towards the same (111)-orientation during cold rolling [2].

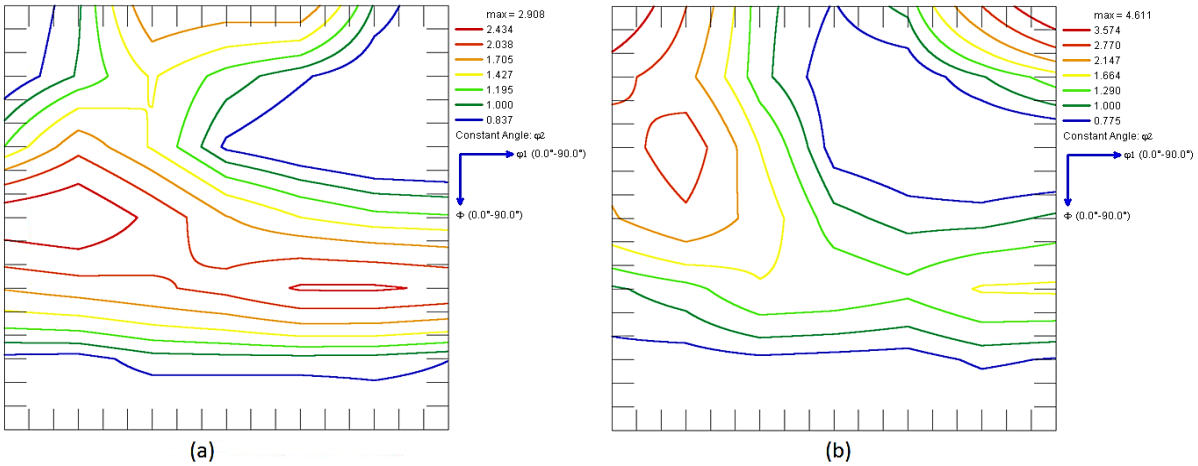

Figure 3. HB-CR rolling ODF texture at section $\varphi_2 = 45°$, (a) IECS and (b) ICCS

The ICCS (HB-CR) sample exhibited a mixture of (001) and (111)-oriented grains. The strong (001)-orientation was presumably inherited from the columnar as-cast grains with an initial (100) <uv0> as-cast texture, and which survived the hot rolling stage as (001) <110> components. Shin et al reported that the ND//<001> orientation of the columnar grains, rotates to the $\{001\} < 110 >$ family orientation after a plane strain compression [3]. The transformation of $\{001\} < 110 >$ to $\{111\} < 112 >$ family orientation is difficult because the $\{001\} < 110 >$ family component has a low Taylor factor and in

turn contains low stored deformation energy, which leads to a slow transformation rate during hot working and, therefore, the $\{001\} < 110 >$ orientation persisted during the cold rolling stage. This could explain the domination of (001)-oriented grains in the ICCS specimen during subsequent cold rolling stage.

3.2. Annealing (HB-CRA) recrystallization texture

The recrystallized texture of IECS was mainly characterized by the γ −fiber texture component while the ICCS revealed clusters of γ −fiber and shifted rotated Goss texture components, figure 4. During recrystallization annealing of the cold rolled IECS, the γ −fibre texture components were strengthened and Cube texture diminished, as shown in figure 4 (a) and figure 3 (a) respectively. Conversely in IECS, the ICCS was characterized by both the γ −fibre and shifted rotated Goss texture components with strong and equal intensities, while the rotated Cube texture emerged relatively weak at 1.528 to 1.699 intensity.

Texture homogeneity was attained by IECS during the recrystallization process. As expected, the ICCS recrystallized into three discrete texture components, namely γ −fiber, rotated Cube and rotated Goss texture components at higher intensities, figure 4. Consequently, this promoted texture inhomogeneity.

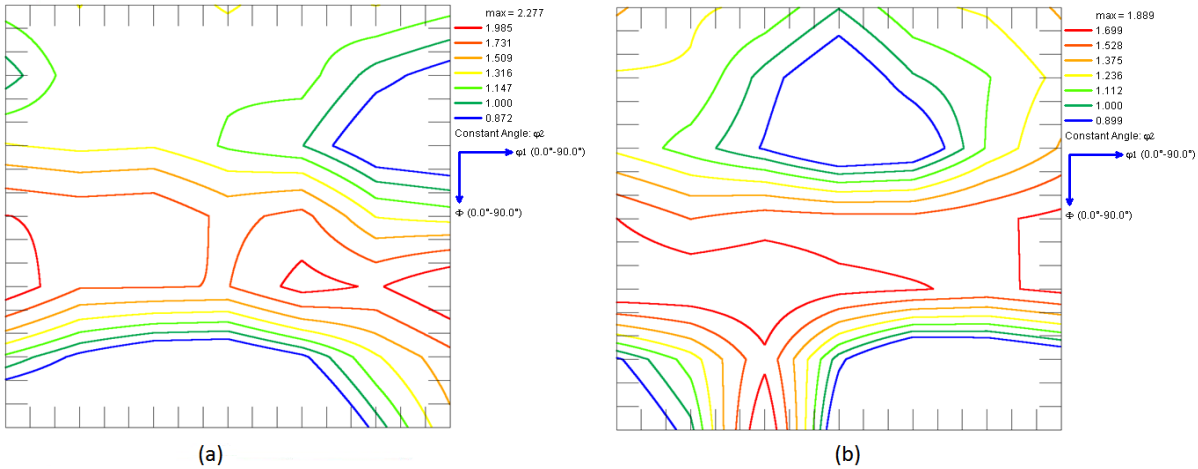

Figure 4. HB-CRA recrystallization texture at section $\varphi_2 = 45°$, (a) IECS and (b) ICCS

Recrystallization nucleation prefers high angle grain boundaries (HAGBs) of deformed grains and the new grains nucleated and grow by consuming the deformed grains while retaining their orientations [4]. In addition, grains with an orientation of high recrystallization rate, such as (111), will nucleate first by adopting that orientation and grow at an expense of other deformed grains with different orientations from (111). However, (100)-orientations are difficult to recrystallize because of their low stored deformation energy and, therefore they survive the scavenging of (111)-oriented grains while others are consumed [5]. This could be an explanation for the textures observed on both IECS versus ICCS in HB-CRA condition.

3.3. Texture effect on mechanical property

Figure 5 presents engineering stress-strain curve of both IECS and ICCS in HB-CRA condition. Both IECS and ICCS exhibited similar yield and ultimate tensile strengths of 270 and 600 MPa respectively, measured in the RD. However, the percentage elongation of the IECS was found to be slightly higher by 1.5% than the ICCS, which is an indication of better drawability.

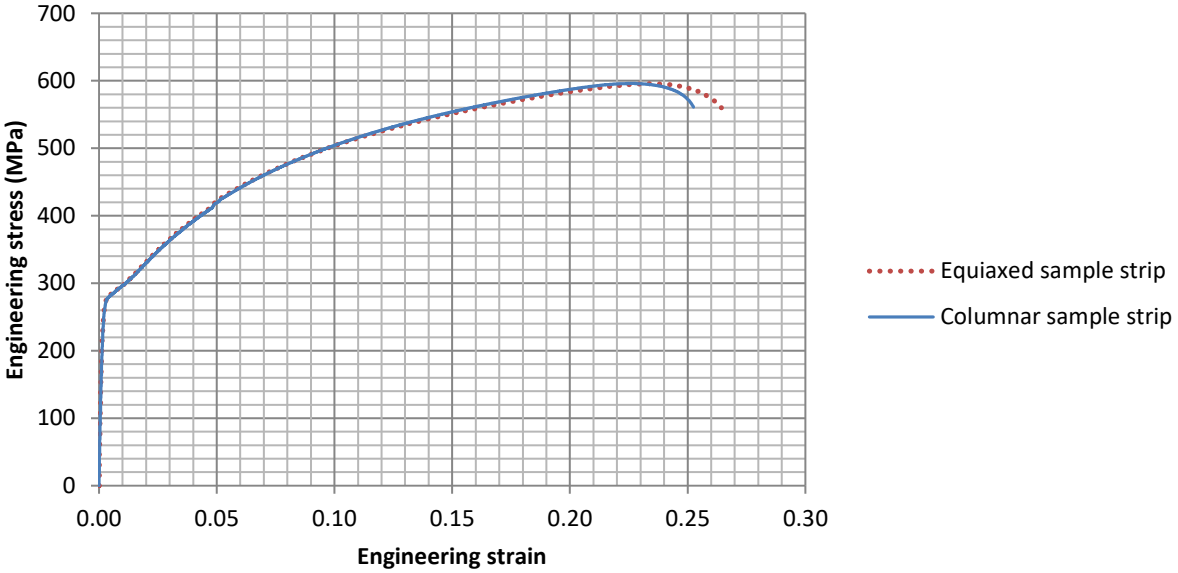

Figure 5. Typical engineering stress-strain curve in HB-CRA condition for IECS and ICCS measured in the RD.

The difference in elongation was attributed to the differences in recrystallization texture between the two samples. Nafisi et al. reported that the plastic deformation response is an anisotropic property i.e. it is influenced by the grains crystallographic texture [5]. A slightly further elongation in IECS was therefore attributed to the homogeneous distribution of recrystallized γ-fibre texture [6, 7]. Raabe et al, Knutsen et al and Zong et al observed that the annealed FSS sheets with prominently γ −fibre texture exhibited higher percentage elongation, and that texture inhomogeneity with orientations other than {111} −texture lowers percentage elongation [8, 9, and 10]. The percentage elongation of IECS material in this study supported findings of Hamada et al. [12] since the co-existence of the Cube and γ −fibre texture components in ICCS material seemed to negatively affect the percentage elongation.

The strength is also an anisotropic property, i.e. the same as elongation; therefore, texture should have an effect on it. Nafisi et al. [5] and Zong et al. [11] argued that the (001) <110> rotated cube components are responsible for the anisotropy in the strength of steel i.e. strongly anisotropic in the 45° and 90° than in the direction 0° angle to the RD. And rotated cube components provide planes that facilitate crack nucleation and propagation across the grains [5]. Therefore, this could explain the similarity in both the yield strength and the UTS measured in the direction of 0° angle to the RD in this work.

4. Conclusions

The effect of the cast structure on the evolution of texture and subsequent mechanical properties in 433 FSS was studied and the following conclusions were made:

- The IECS and ICCS cast structures influence the development of crystallographic texture differently during cold rolling and annealing processes. The IECS promoted homogeneous γ −fiber texture while ICCS promoted heterogeneous texture components with a predominance of γ −fiber, Goss and α −fiber texture components.
- The homogeneous γ −fiber texture components in IECS marginally increased the percentage elongation whereas the inhomogeneous texture in ICCS effected it negatively.

5. Acknowledgements

The authors are grateful to Mintek for the financial support and laboratory facilities, University of Pretoria for the administration, laboratory and study facilities and Columbus Stainless for the supply of material and technical support.

6. References

[1] Raabe, D. 1994. Texture of the strip cast and hot rolled ferritic and austenitic stainless steels. Material science, The institute of materials, The Institute of materials, Manuscript received 24 February 1994, final form in 16 May 1994, The institute of Metallkunde and Metallphysik, RWTH Aachen, Aachen Germany.

[2] Patra, S and Singhal, L.K. 2013. Influence of hot band annealing and cold rolling on texture and ridging of 430 stainless steel containing aluminium. Material sciences and applications, volume 4, pp 70-76.

[3] Shin. H.J, AN. J.K, Park. S.H, and Lee. D.N. 2003. The effect of texture on ridging of ferritic stainless steel. Acta Materialia 51, pp 4693-4706.

[4] Hamada, J., Matsumoto, Y, Fudanodef, and Maeda, S. 2003. Effect of initial solidification on ridging phenomenon and texture in type 430 ferritic stainless steel sheets. ISIJ International, Vol 43, no 12, pp 1989-1998.

[5] Nafisi. S, Arafin. M.A, Collins. L, AND Szpunar. J. 2012. Texture and mechanical properties of API X100 steel manufactured under various thermos-mechanical cycles. Material Science and Engineering A 531 (2012), pp 2-11.

[6] Choi. J. H, Choi. J. Y, Kim. J. C, Kim. J. J, and Kim. S. K. 2009. Control of columnar to equiaxed transition in continuous casting of 16% Cr Ferritic Stainless Steel. POSCO, Korea, Metallurgical Italian, September 2009.

[7] Blandford. P. 1989. Through thickness inhomogeneity of steel-sheet texture and its effect on material properties. A thesis submitted to the Faculty of Graduate Studies and Research in Partial Fulfilment of the requirements for the degree of Masters of Engineering, Department of Mining and Metallurgical Engineering, McGill University, Montreal Canada, November 1989.

[8] Raabe. D, Lee. J, H, Young. M, Engler. O and Park. S. 2005. Effect of through-thickness Macro- and Micro-texture gradient on ridging of 17% Cr Ferritic Stainless Steel Sheet. Division of Materials Science and Engineering, Korea University, Seoul, Korea. Steel research int 76, Vol no.11, pp 797-806.

[9] Knutsen. R.D and Wittridge. N.J. 2002. Modelling surface ridging in ferritic stainless steel. Centre for Material Engineering, Department of Mechanical Engineering, University of Cape Town, 7701 Rondebosch, RSA.

[10] Lioyd. D.J, Wu. P.D. and Huang. Y. 2006. Correlation of ridging and texture in ferritic stainless steel sheet, Department of Mechanical Engineering, McMaster University Hamilton, Ont, Canada. Material Science and Engineering A 427 (2206), pp 241-245.

[11] Zong. C, Zhu. G and Mao. W. 2013. Effect of crystallographic texture on anisotropy of yield strength in API X 100 pipeline steel. Journal of Iron and Steel research, international 2013, 20(8), pp 66-71.

[12] Hamada. J.I., Inoue. H. and Ono. N. 2011. Effect of texture on R-value of ferritic stainless steel sheets. Steel Research Laboratories, Nippon Steel Corporation, 20-1 Shintomi, Futsu, Chiba, 293-8511, Japan, Department of Material Science, Graduate School of Engineering, Osaka Prefecture University, 1-1 Gakuen-Cho, Naka-ku, Sakai, Osaka, 599-8531, Japan.